The Canadian Mineralogist
Vol. 37, pp. 525-541 (1999)

DEFORMATION OF SILICATE GARNETS: BRITTLE–DUCTILE TRANSITION AND ITS GEOLOGICAL IMPLICATIONS*

ZICHAO WANG[1] AND SHAOCHENG JI[1]

Département de Géologie, Université de Montréal, Case postale 6128, succursale Centre-Ville, Montréal, Québec H3C 3J7

Abstract

To understand the deformation behavior of silicate garnets, we performed experiments on six representative silicate garnets at temperatures (T) of 1173–1673 K, strain-rates ($\dot{\varepsilon}$) of 10^{-7}–10^{-4}/s and well-controlled thermodynamic conditions. On the basis of mechanical data, microstructures and the comparison between experimental results with deformation of natural garnets, this study yields three new insights into the deformation behavior of silicate garnets. (1) The critical temperature (T_c) for the brittle–ductile transition of garnet deformation, in terms of melting temperature (T_m) and strain-rate ($\dot{\varepsilon}$), can be described by an empirical equation: $T_c = T_m$ [(1.043 ± 0.032) + (0.030 ± 0.001)log($\dot{\varepsilon}$)]. In the ductile regime, where $T > T_c = T_m$ [1.075 + 0.029log($\dot{\varepsilon}$)], steady-state creep of garnets follows a power law: $\dot{\varepsilon} = A\left(\frac{\sigma}{\mu}\right)^n \exp\left(-g\frac{T_m}{T}\right)$, where $n = 3.0 \pm 0.5$, ln$A$(/s) = 40.1 ± 5.6, g = 32 ± 2, σ is the flow stress at steady-state creep, and μ is shear modulus of garnet. (2) A microstructural investigation suggests that crystal plasticity, enhanced by the activation of dislocation glide (slip systems ½<111>{1$\bar{1}$0}), is responsible for the brittle–ductile transition. (3) Extrapolation of the experimental results to geological strain-rates (10^{-16}–10^{-14}/s) suggests that the brittle–ductile transition of silicate garnets in nature occurs at $T > 0.65$–$0.70\ T_m$. This indicates that crustal garnets such as almandine, pyralspite and grossular can be deformed in ductile fashion under extremely high temperature ($T > 1123$ K). The extrapolation also shows that in the crust, garnet (*e.g.*, "pyralspite") is much stronger than quartz and feldspar at temperature lower than 1123 K, but the rheological contrast of garnet with quartz and particularly with feldspar is minimal at temperature higher than 1123–1173 K. In the upper mantle, however, pyrope is invariably about two orders of magnitude stronger than olivine, and the rheological contrast between these two minerals is almost constant. We conclude that silicate garnets are mostly rigid and brittle in the crust, but ductile as long as the conditions of high temperature and low strain-rate are satisfied.

Keywords: silicate garnet, brittle–ductile transition, flow law, high-temperature deformation, dislocation creep.

Sommaire

Afin de mieux comprendre le comportement des grenats silicatés au cours d'une déformation, nous avons effectué une série d'expériences avec six compositions représentatives sur l'intervalle de température compris entre 1173 et 1673 K, à des taux de déformation de 10^{-7} à 10^{-4}/s et des conditions thermodynamiques bien définies. A la lumière de données mécaniques, des microstructures et d'une comparaison des résultats expérimentaux avec la déformation dans les grenats naturels, nous en arrivons à trois perceptions nouvelles du comportement d'un grenat silicaté au cours de la déformation. (1) On peut décrire la température critique T_c de la transition entre comportement ductile et comportement cassant d'un grenat en termes de la température de fusion T_m et du taux de déformation, selon l'équation empirique suivante: $T_c = T_m$ [(1.043 ± 0.032) + (0.030 ± 0.001)log($\dot{\varepsilon}$)]. Si la déformation se déroule dans le domaine ductile, dans lequel $T > T_c = T_m$ [1.075 + 0.029log($\dot{\varepsilon}$)], le fluage stationnaire d'un échantillon de grenat répond à une loi puissance: $\dot{\varepsilon} = A\left(\frac{\sigma}{\mu}\right)^n \exp\left(-g\frac{T_m}{T}\right)$, dans laquelle $n = 3.0 \pm 0.5$, ln$A$(/s) = 40.1 ± 5.6, g = 32 ± 2, σ est la contrainte de fluage aux conditions de fluage stationnaire, et μ est le module de cisaillement du grenat. (2) Une étude microstructurale fait penser que la plasticité d'un cristal, renforcie par l'activation du glissement des dislocations selon le mécanisme de glissement ½<111>{1$\bar{1}$0}, serait responsable de la transition de régime cassant à régime ductile. (3) D'après une extrapolation des résultats expérimentaux à des taux de déformation géologiquement réalistes (10^{-16}–10^{-14}/s), la transition de régime cassant à régime ductile dans les grenats silicatés dans la nature se situerait à une température supérieure à 0.65–$0.70\ T_m$. C'est donc dire que dans la croûte, les grenats comme l'almandine, les grenats pyralspitiques et le grossulaire ne peuvent se déformer de façon ductile qu'à température extrêmement élevée ($T > 1123$ K). L'extrapolation montre aussi que dans la croûte,

* LITHOPROBE contribution number 1020.

[1] *E-mail addresses*: wangzi@magellan.umontreal.ca, jish@ere.umontreal.ca

le grenat, par exemple pyralspitique, est beaucoup plus robuste que le quartz et le feldspath à une température inférieure à 1123 K, mais le contraste rhéologique entre le grenat et le quartz, et particulièrement avec le feldspath, est très faible à une température supérieure à 1123–1173 K. Dans le manteau supérieur, par contre, le pyrope est systématiquement environ deux ordres de grandeur plus robuste que l'olivine, et le contraste rhéologique entre ces deux minéraux est à peu près constant. Nous pensons que les grenats silicatés sont surtout rigides et cassants dans la croûte, mais ils peuvent devenir ductiles dans les milieux de température élevée et de faible taux de déformation.

(Traduit par la Rédaction)

Mots-clés: grenat silicaté, transition du régime cassant au régime ductile, loi de fluage, déformation à température élevée, fluage stationnaire des dislocations.

Introduction

Garnet is a widespread metamorphic mineral in the middle and lower crust, and is likely to be one of the major constituents in the subducting oceanic crust and the mantle transition zone (Ringwood 1991). Although silicate garnets are usually considered as rigid (undeformable) or brittle in the crust and the uppermost mantle, garnet subjected to plastic deformation has been reported (Dalziel & Bailey 1968, Ross 1973, Ando *et al.* 1993, Ji & Martignole 1994, Doukhan *et al.* 1994, Ingrin & Madon 1995). The conditions of brittle–ductile transition for garnet-group minerals remain as a question to be answered. This experimental investigation was designed to address this theme.

Background Information

In their studies of high-grade felsic mylonites, Dalziel & Bailey (1968), Ross (1973), Gregg (1978), Ji & Martignole (1994) and Kleinschrodt & McGrew (1995) observed that grains of garnet form ellipsoids with the shortest axis normal to the mylonitic foliation and axial planes of folds. Some garnet crystals even show pinch-and-swell structures rather than brittle boudinage. Because garnet grains are equidimensional prior to deformation, present shapes suggest that they are porphyroclasts that were tectonically deformed where no grain-boundary migration occurred. The following features are particularly noted: (1) Crystals of garnet in a matrix of quartz are more strongly deformed than those in a matrix of feldspar (Ji & Martignole 1994, Kleinschrodt & McGrew 1995). This phenomenon has been explained using the shear-lag model (Ji *et al.* 1997). (2) Feldspar grains have similar aspect-ratios to coexisting grains of garnet, indicating that the rheological contrast between these two minerals is minimal during their deformation at high temperature (Ji & Martignole 1994). (3) Observations made by transmision electron microscopy (TEM) (Ji & Martignole 1994) demonstrate that subgrain boundaries and networks of dislocation are extensively developed in the ellipsoidal grains of garnet. Dislocation climb thus is efficient. (4) Indirect evidence of dislocation cells and considerable distortion of the crystal structure in the oblate grains of garnet has been provided by Dalziel & Bailey (1968) and Ross (1973) on the basis of strong asterism and splitting of spots in Laue photographs. (5) Laue X-ray diffraction (Dalziel & Bailey 1968, Ross 1973) and analysis of electron-channeling patterns in scanning electron microscopy (SEM) (Kleinschrodt & McGrew 1995) show that flattened or elongate grains of garnet have no marked preferred crystallographic orientation. Ji & Martignole (1996) provided the explanation of this phenomenon.

Ductile garnet has also been found in deformed garnet peridotites. For example, crystals of garnet in garnet peridotite (Almklovdalen, Norway) are elongate parallel to the fold axis of folded layers of peridotite (Bryhni 1966). Carstens (1969) observed that grains of garnet in garnet peridotites are commonly flattened. Grains of garnet in the Norwegian peridotites (Lappin 1967) and in the coesite-bearing eclogites (Su–Lu ultra-high pressure belt, China: Ji *et al.* 1998) are recrystallized. Subgrain boundaries and cell structures were revealed in pyrope (Norwegian and Czech garnet peridotites, Carstens 1969, 1971). The cells, which are defined as small irregular regions misoriented from each other by 2–3°, bounded by walls of dislocation tangles, are interpreted as a result of dislocation interactions of several active slip systems.

There have been several TEM studies on naturally deformed garnet from the upper mantle. Doukhan *et al.* (1994) investigated ultradeep (>300 km, 13 GPa and 1473 K) pyrope-rich garnet from the Jagersfontein kimberlite pipe (South Africa). They found that dislocations are organized along regularly spaced subgrain boundaries. The density of free dislocations is still as high as 10^{11} m^{-2} within these subgrains. Most of dislocations have a Burgers vector (**b**) of ½<111>, but a few dislocations have Burgers vectors of <100> or <110>. TEM observations by Ando *et al.* (1993) showed that grains of garnet from garnet peridotites and eclogites are deformed by slip and climb of dislocations with **b** = ½<111> and **b** = <100>. They concluded that the slip direction of active dislocations may change with differential stress: **b** = <100> appears under lower differential stress, whereas **b** = ½<111> occurs under higher differential stress. These studies demonstrate that climb-accommodated dislocation creep is likely the dominant

mechanism in the plastic deformation of silicate garnet in nature.

All the observations suggest that silicate garnet, compared to coexisting minerals, is stronger and more brittle, but can be ductile at certain conditions. However, the nature and mechanisms of brittle–ductile transition in silicate garnets have not been studied in detail (Smith 1982, Ingrin & Madon 1995, Drury & Fitz Gerald 1997), although oxide garnets such as $Y_3Fe_5O_{12}$ (YIG: Rabier *et al.* 1976, Rabier 1979, Rabier *et al.* 1979, Karato *et al.* 1995), $Gd_3Ga_5O_{12}$ (ΓGG: Rabier & Garem 1984, Garem *et al.* 1982, Wang *et al.* 1996a), and $Y_3Al_5O_{12}$ (YAG: Parthasarathy *et al.* 1992, Corman 1990, Karato *et al.* 1994, Blumental & Philips 1996) have been extensively investigated. For a better understanding of the brittle–ductile transition, we conducted a systematic experimental study on six silicate garnets. This study is focused on the effects of temperature and strain-rate on the onset of crystal plasticity. In this paper, we will present our experimental results and discuss the role of crystal plasticity in determining brittle–ductile transition of silicate garnets. Finally, geological and geophysical implications of these findings are discussed.

Experimental Details

Starting crystals

Silicate garnets have a body-centered cubic structure with variable chemical composition. Winchell (1933), in a study of the garnet composition from different environments, divided common garnets into two groups, ugranditic and pyralspitic, within which complete solid-solution exists but between which a compositional gap seems evident (Meagher 1982). The general formula for the ugranditic garnet group is $Ca_3Y_2Si_3O_{12}$, with Cr^{3+} (uvarovite), Al^{3+} (grossular) and Fe^{3+} (andradite) as the most common cations occupying the octahedrally coordinated *Y*-site. For the pyralspitic group, the general formula is $X_3Al_2Si_3O_{12}$, in which the triangular dodecahedron *X* site is commonly occupied by Mg^{2+} (pyrope), Fe^{2+} (almandine) and Mn^{2+} (spessartine). We selected six single crystals from samples of these two groups, commercially available from Wards Scientific (Rochester, N.Y.) and Palla Properties (California). All selected crystals are of gem quality, and free of microcracks and visible inclusions. They are either rhombic dodecahedral or icositetrahedral in crystal form, between 6 and 10 mm in diameter. Electron-probe micro-analyses indicate that they are grossular (Grs), ferrian grossular (Grs_Fe), almandine (Alm), pyralspite (Prpalmsps), spessartine (Sps) and uvarovite (Uv) (Table 1). The starting crystals were examined under the optical microscope and by transmission electron microscopy. We did not observe any clear sign of deformation, such as shear bands, undulatory extinction and twinning at an optical scale. Dislocations were rarely observed, and the density of dislocations is estimated to be lower than $10^9/m^2$.

TABLE 1. CHEMICAL COMPOSITION, MELTING TEMPERATURE (T_m), SHEAR MODULUS AND SOURCE OF SILICATE GARNET SAMPLES STUDIED IN THIS WORK

Sample	Composition	μ (GPa)	T_m (K)	Source
Grossular (Grs)	$Ca_3(Al_{0.96}Ti_{0.04})_2Si_3O_{12}$	106*	1522*	1
Ferrian grossular (Grs_Fe)	$Ca_3(Al_{0.9}Fe_{0.1})_2Si_3O_{12}$	109*	1510*	1
Almandine (Alm)	$(Fe_{0.86}Mg_{07.0}Ca_{0.06})_3Al_2Si_3O_{12}$	93**	1540**	2
Pyralspite*** (Prpalmsps)	$(Mg_{0.52}Mn_{0.22}Fe_{0.18}Ca_{0.08})_3Al_2Si_3O_{12}$	98*	1670*	1
Spessartine (Sps)	$Mn_3Al_2Si_3O_{12}$	96*	1470*	3
Uvarovite (Uv)	$Ca_3Cr_2Si_3O_{12}$	85*	1560**	3

* From Karato *et al.* (1995). ** This study. *** This garnet is also referred to as "rhodolite" in the literature. 1. Unknown locations, purchased from Palla Properties (California); 2. Hebei, People's Republic of China; 3. Unknown locations, purchased from Wards Co. (Rochester, New York). Mineral symbols used in this paper are from Kretz (1983).

Experimental procedure

Crystals to be tested were prepared as rectangular parallelepipeds with dimension of 2.5 × 2.5 × 5.0 mm^3. Because ½<111> is the shortest Burgers vector and dislocations with **b** = ½<111> are commonly observed in natural garnets, crystals were oriented such that the long axis ($//\sigma_1$) is parallel to <100>. This orientation favors the activation of ½<111>{110} slip systems. To avoid potential chemical reaction between garnet samples and the SiC pistons, the samples were sandwiched between two YAG platens (<110> axis parallel to the compression axis) with a sectional area at least ten times larger than that of sample. These platens were then placed between two Al_2O_3 platens (corundum with <001> axis parallel to the compression axis, Fig. 1). We verified by calibration that deformation of this assembly (Al_2O_3, YAG platens and SiC piston) was significantly smaller than that of the sample (<5% of total strain) within the temperature range of deformation. Neither reaction between samples and YAG nor decomposition of the garnet sample was observed after deformation under the conditions of this study.

All experiments were performed at temperatures in the interval 1173–1673 K in a well-controlled environment by flowing mixture of CO–CO_2. Servo-controlled testing machines incorporating a vertically mounted high-temperature furnace were employed in this study. Temperature was measured by two R-type thermo-

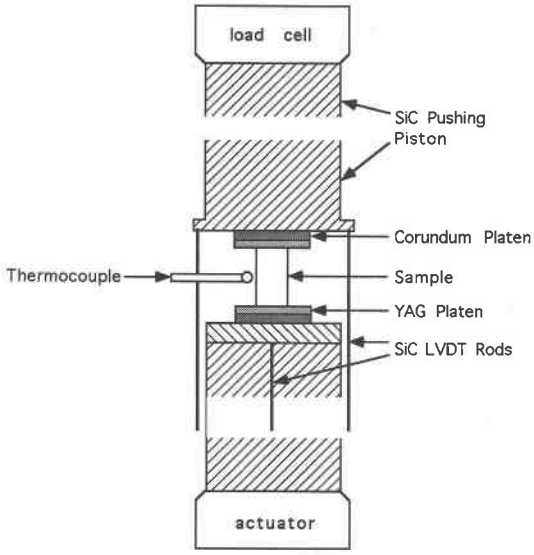

FIG. 1. Schematic drawing of the sample assembly (not to scale).

couples (Pt–13%Rh *versus* Pt) and controlled within ±1 K during a run. Most of tests were made in a constant-displacement rate mode (strain rate $\dot{\varepsilon} = 10^{-7}$/s to 10^{-4}/s). Stresses were calculated from force data measured with a load cell, which gives an accuracy of 0.5% at a full-scale cartridge (200–500 kg). Displacement was monitored by two sets of linear variable differential transformers (LVDT), with a resolution of ~10^{-4} mm. Stress–strain curves, shown hereafter, were corrected for instrument stiffness and change in cross-section of samples. We assumed a constant volume of crystals during deformation.

After deformation, samples were cut into two or three pieces along either their slip planes or normal to them for optical and TEM observations. Carbon-coated foils were examined with a JEOL–200 CX electron microscope operated at an accelerating voltage of 200 kV. We did not see a second phase in the deformed samples at a resolution of 0.1 μm, and thus no decomposition or melting occurred during the experiments.

Criteria for brittle–ductile transition

This study was concerned mainly with the brittle–ductile transition of garnet crystals. The term "ductility" is used here to denote the capacity for a substantial plastic deformation of the crystal without gross fracturing. This definition is an essentially macroscopic or phenomenological one, but is combined with a mechanism of deformation whereby the plastic deformation occurs merely through crystal plasticity. The change in deformation behavior from macroscopic fracture to homogeneous plastic flow is taken as defining the brittle–ductile transition. In particular, following Heard (1960), Heard & Carter (1968) and Evans *et al.* (1990), the value of 3–5% plastic strain (ε_p) to failure is taken as defining the transition. Taking ε_p as a quantitative criterion, the brittle–ductile transition boundary is constructed in terms of temperature and strain-rate at room pressure.

EXPERIMENTAL RESULTS

Mechanical data

Table 2 summarizes experimental conditions and mechanical data from experiments successfully completed. A schematic stress-strain ($\sigma - \varepsilon$) curve is illustrated in Figure 2. Garnet crystals, in general, show three stages of deformation: (1) linear deformation (OA along the $\sigma - \varepsilon$ curve), (2) nonlinear deformation (strain-hardening, AB along the $\sigma - \varepsilon$ curve). The stress, measured at yield point (A), is defined as yield stress σ_y. (3) Post-peak deformation (BC in $\sigma - \varepsilon$ curve). The deformation of garnet crystals is characterized by a high yield-point close to peak stress (σ_p is measured at point B in Fig. 2, which is an indicator for the difficulty of plastic deformation). After peak stress, a stress drop commonly occurs, and garnet crystals undergo either fracturing (crystal failure at point X after limited strain) or steady-state deformation depending on temperature and strain rate. Representative stress–strain curves for Prpalmsps, Grs and Sps are shown in Figure 3. It can be seen that

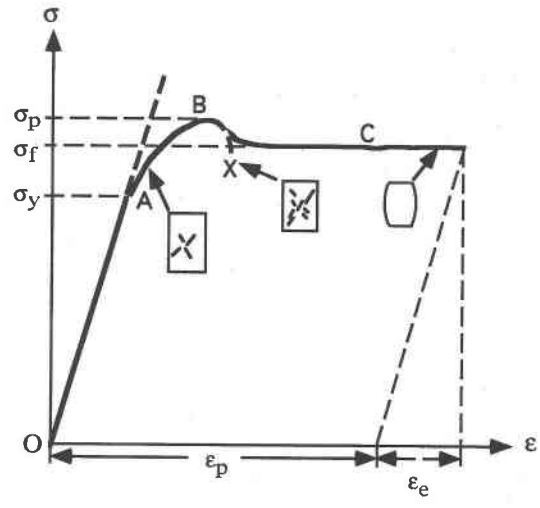

FIG. 2. Schematic diagram illustrating typical stress–strain pattern and macroscopic appearance of deformed samples. A: yield point, B: peak stress, X: the point at which a sample fails, C: steady-state flow.

TABLE 2. EXPERIMENTAL CONDITIONS AND RESULTS FOR CRYSTALS COMPRESSED ALONG THE <100> DIRECTION

Run No.	T (K)	$\dot{\varepsilon}$ (s^{-1})	Stress (MPa)[1] σ_y	σ_p	σ_f	ε_p (%)[2]	Deformation behavior
Alm1-d2	1223	1.0×10^{-6}		380		1.1	brittle[3]
Alm1-d3	1248	1.8×10^{-5}		440		2.4	brittle
Alm1-d4	1273	4.5×10^{-6}	335	550		3.4	brittle
Alm2-d5	1323	1.0×10^{-5}		570		4.2	brittle
Alm2-d7	1323	3.2×10^{-6}	275	490		5.1	semi-brittle[4]
Alm2-d9	1323	1.0×10^{-6}	250	465		5.7	semi-brittle
Alm3-d10	1348	1.0×10^{-5}		520		5.6	semi-brittle
Alm3-d12	1373	1.0×10^{-6}	140	230	220 ± 15	7.9	ductile[5]
Alm4-d13	1373	5.6×10^{-6}	245	410	405 ± 24	8.6	ductile
Alm4-d15	1423	5.0×10^{-5}	320	498	495 ± 20	7.1	ductile
Alm5-d17	1423	1.6×10^{-5}	200	385	380 ± 19	7.5	ductile
Alm6-d19	1423	1.0×10^{-6}	102	115	90 ± 11	8.5	ductile
Alm6-d20	1473	1.6×10^{-6}	105	120	110 ± 13	7.8	ductile
Prpalmsps1-d3	1323	1.0×10^{-7}		360		2.3	brittle
Prpalmsps1-d5	1348	2.5×10^{-6}	460	470		3.2	brittle
Prpalmsps2-d7*	1373	1.0×10^{-6}	390	425		1.5	brittle
Prpalmsps2-d8	1373	5.0×10^{-7}		345		3.4	brittle
Prpalmsps3-d9	1373	1.6×10^{-7}		278		2.5	brittle
Prpalmsps3-d10	1398	1.8×10^{-7}		302		5.1	semi-brittle
Prpalmsps4-d11*	1423	1.0×10^{-6}	275	285		4.0	semi-brittle
Prpalmsps4-d13	1423	5.4×10^{-7}	170	195		4.6	semi-brittle
Prpalmsps5-d14	1473	8.5×10^{-7}	215	226	200 ± 15	6.8	ductile
Prpalmsps5-d16*	1513	7.0×10^{-7}	167	180	167 ± 16	10.5	ductile
Prpalmsps6-d17	1503	2.4×10^{-6}	220	250	260 ± 20	7.3	ductile
Prpalmsps7-d18	1503	5.0×10^{-7}	150	160	160 ± 8	8.2	ductile
Prpalmsps8-d20	1528	2.1×10^{-6}	142	215	213 ± 21	9.0	ductile
Sps1-d2*	1323	1.0×10^{-6}	290	305		1.5	brittle
Sps2-d4	1373	4.0×10^{-6}		364		2.8	brittle
Sps3-d9	1236	3.2×10^{-8}				3.1	semi-brittle
Sps3-d5*	1423	1.0×10^{-6}	110	146		3.0	semi-brittle
Sps4-d6	1423	4.0×10^{-7}	50	74	60 ± 6	6.8	ductile
Sps5-d7*	1448	1.0×10^{-6}	100	130	107 ± 12	6.5	ductile
Grs_Fe1-d2	1273	1.0×10^{-5}		380		2.5	brittle
Grs_Fe1-d3	1273	1.0×10^{-6}	350	360		3.4	brittle
Grs_Fe2-d4	1323	1.0×10^{-5}		321		1.8	brittle
Grs_Fe2-d6	1323	3.1×10^{-6}	270	294		2.8	brittle
Grs_Fe3-d7	1373	1.0×10^{-5}	220	265		5.2	semi-brittle
Grs_Fe6-d13	1356	3.1×10^{-5}		334		3.4	semi-brittle
Grs_Fe6-d14	1392	1.0×10^{-4}		410		4.2	semi-brittle
Grs_Fe3-d8	1373	1.0×10^{-6}	210	218	206 ± 23	7.8	ductile
Grs_Fe4-d10	1423	1.0×10^{-5}	125	306	305 ± 15	8.7	ductile
Grs_Fe4-d11	1423	5.0×10^{-6}	136	245	240 ± 13	9.5	ductile
Grs_Fe5-d12	1423	1.8×10^{-6}	121	175	170 ± 8	9.4	ductile
Grs1-d3	1273	6.3×10^{-7}		410		1.9	brittle
Grs2-d4	1323	1.0×10^{-6}	360	370		2.0	brittle
Grs2-d6*	1348	1.0×10^{-6}	300	327		3.0	brittle
Grs3-d7	1350	1.0×10^{-6}		341		2.9	brittle
Grs4-d8	1351	1.0×10^{-6}	250	287		3.4	brittle
Grs5-d10	1398	1.0×10^{-5}		289		5.0	semi-brittle
Grs5-d11*	1383	5.6×10^{-7}	145	170		4.3	semi-brittle
Grs8-d19	1258	3.2×10^{-8}		340		3.2	semi-brittle
Grs6-d12	1398	5.6×10^{-7}	135	154	149 ± 13	8.2	ductile
Grs6-d13	1398	2.5×10^{-7}	115	126	115 ± 11	6.8	ductile
Grs7-d15*	1473	1.0×10^{-6}	70	85	83 ± 9	7.5	ductile
Grs7-d17	1423	3.2×10^{-7}	81	98	94 ± 6	6.5	ductile
Uv1-d1	1313	2.0×10^{-6}		290		1.4	brittle
Uv1-d5	1373	1.0×10^{-7}		150		3.4	semi-brittle
Uv5-d6	1388	1.0×10^{-6}		220		4.3	semi-brittle
Uv2-d2	1373	1.0×10^{-6}	220	240		3.9	semi-brittle
Uv3-d3	1373	5.0×10^{-7}	150	170	165 ± 16	6.5	ductile
Uv4-d4	1423	1.0×10^{-6}	120	146	140 ± 14	7.1	ductile

[1] The symbols σ_y, σ_p and σ_f refer to yield, peak and flow stresses, respectively. [2] Refers to plastic strain at the end of the experiments. For samples deformed in the brittle and semi-brittle regimes, it is the ultimate plastic strain at which fracture occurred. [3] Fracture occurred at the end of experiment with $\varepsilon_p < 3\%$. [4] Fracture occurred at the end of the experiments with $3\% < \varepsilon_p < 5\%$. [5] No fracture was observed at the end of the experiments, $\varepsilon_p > 5\%$.

deformation of these garnets is very sensitive to T and $\dot{\varepsilon}$. The crystals are very strong and brittle, even at fairly high temperature (~0.8T_m; T_m: melting temperature). All three samples of garnet show a remarkably linear deformation up to 0.5–0.8% strain; crystals do not yield until the applied stress reached close to peak stress. Brittle fracture occurred just after peak stress (ε_p < 1–3%). With increasing T (>0.8 T_m) or decreasing $\dot{\varepsilon}$ (<10^{-6} s^{-1}), or both, garnet crystals yield at relatively low stress, and plastic strain after the yield point becomes more pronounced. Taking sample Prpalmsps as an example (see Fig. 3a), it yielded at 70–80% of peak stress and reached a "steady-state" deformation when deformed at 1423 K and $\dot{\varepsilon} = 10^{-6}$/s. Fracture occurred at a plastic strain ~4% of ε_p. Sample Prpalmsps reached steady-state deformation, and no fracture was observed at a plastic strain as large as $\varepsilon_p = 10\%$ (ε_p is measured at the end of the experiment), when it was deformed at T = 1513 K and $\dot{\varepsilon} = 7 \times 10^{-7}$/s. Similar behavior was observed for the other silicate garnets (see Figs. 3b and 3c for Grs and Sps). Observations on mechanical behavior indicated that silicate garnets underwent a complete spectrum of deformation (from brittle to ductile) as deformation conditions were changed.

Experimental data are summarized in a $T/T_m - \dot{\varepsilon}$ diagram (Fig. 4) to determine $T - \dot{\varepsilon}$ conditions for transition from brittle fracture to ductile flow. We considered deformation as brittle and semi-brittle if fracturing occurred eventually at $\varepsilon_p < 3\%$ and $\varepsilon_p = 3$–5%, respectively, but ductile if no fracture was observed at $\varepsilon_p >$ 6% (at the end of an experiment). As shown in Figure 4, brittle fracture is gradually replaced by plastic flow with increasing T or decreasing $\dot{\varepsilon}$ (or both) for both pyralspitic and ugranditic garnets. Within the range of strain rates in this study, the transition starts at a temperature in the range 0.80–0.85 T_m and 0.83–0.90 T_m for pyralspitic and ugranditic garnets, respectively. To understand further the dependence of the brittle–ductile transition on temperature, we plotted ultimate plastic strain (ε_p) as a function of normalized temperature (T/T_m) at a strain rate of ~10^{-6}/s for both pyralspitic and ugranditic garnets (Fig. 5). The ultimate plastic strain remains small (< 3%) until temperature exceeds 0.80 T_m for pyralspitic garnets and 0.83 T_m for ugranditic garnets. The ultimate plastic strain increased substantially above this temperature, and fracture was effectively suppressed at T > 0.86 T_m, at which ductile flow was observed for both groups. In this context, ultimate plastic

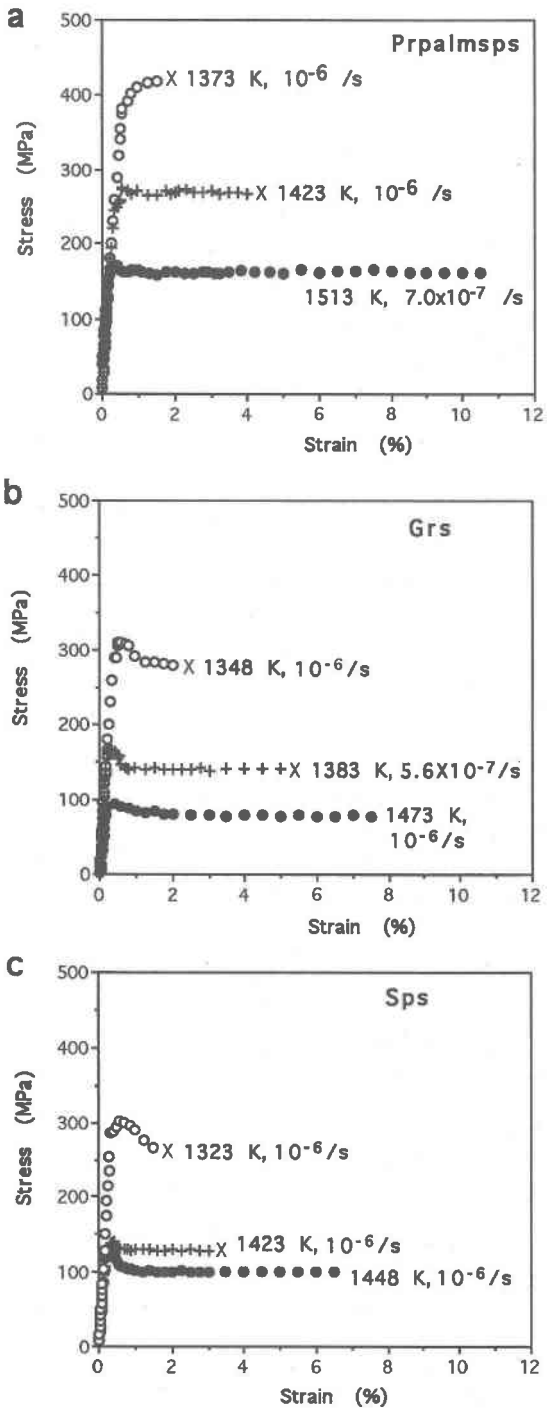

FIG. 3. Stress–strain curves for pyralspitic garnet (a), grossular (b), and spessartine (c). X: the point at which samples fail. Conditions of deformation are given in the figure. See text for more explanations.

strain refers to the permanent strain measured at fracturing. It refers to total plastic strain of samples without fracturing.

In order to determine whether the enhancement in plastic strain with temperature is due to dislocation motion, we studied the strength of ½<111> slip system by assuming that this slip system was activated. The strength of a particular slip system is conventionally expressed in terms of the CRSS (Critical Resolved Shear Stress, τ_c). The CRSS for a given slip system is generally determined from the yield behavior indicated in $\sigma - \varepsilon$ curves of deformed single crystals *via* the relation

$$\tau_c = \sigma_y S \qquad (1)$$

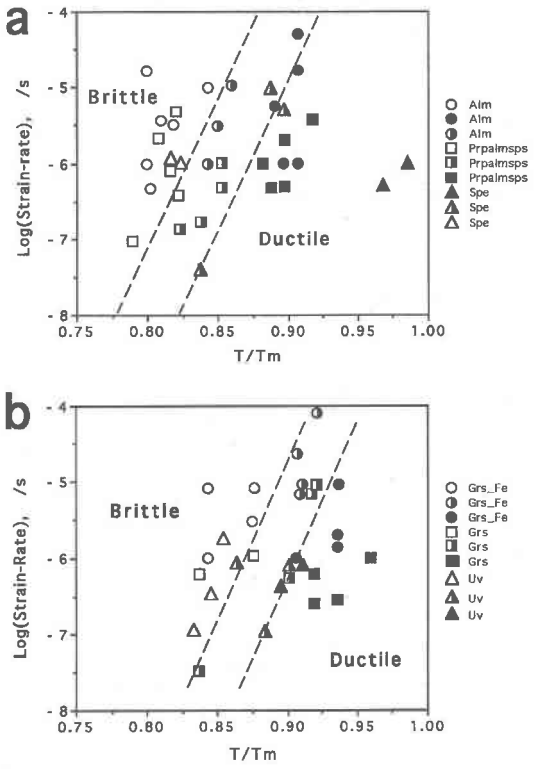

FIG. 4. Variations in deformation behavior of silicate garnets with temperature and strain rate. Open symbols indicate brittle deformation; failure occurs at a permanent strain of $\varepsilon_p < 3\%$. Half-open symbols indicate semi-brittle behavior; failure occurs at a permanent strain ε_p = 3–5%. Solid symbols indicate ductile flow, no fracture observed at the end of experiments, with total plastic strain $\varepsilon_p > 5$–8%. (a) Pyralspitic garnet group, (b) ugranditic garnet group. Dashed lines are schematic and were drawn to show the transition zone.

in which S is the Schmid factor for the active slip system (S = 0.41 for the ½<111>{110} slip system). The CRSS (τ_c) for slip on ½<111> slip systems for silicate garnets, calculated from the yield stress at strain rates of $(1 - 3) \times 10^{-6}$/s, is presented as a function of temperature (Fig. 6). It can be seen that the CRSS decreases rapidly with increasing temperature up to 0.9 T_m. The coincidence in the temperature dependence of τ_c and ε_p suggests that the enhancement in ε_p is related to decrease in CRSS, which makes the intensive motion of dislocations possible. Similar variation of CRSS values with temperature was observed for other garnets as well.

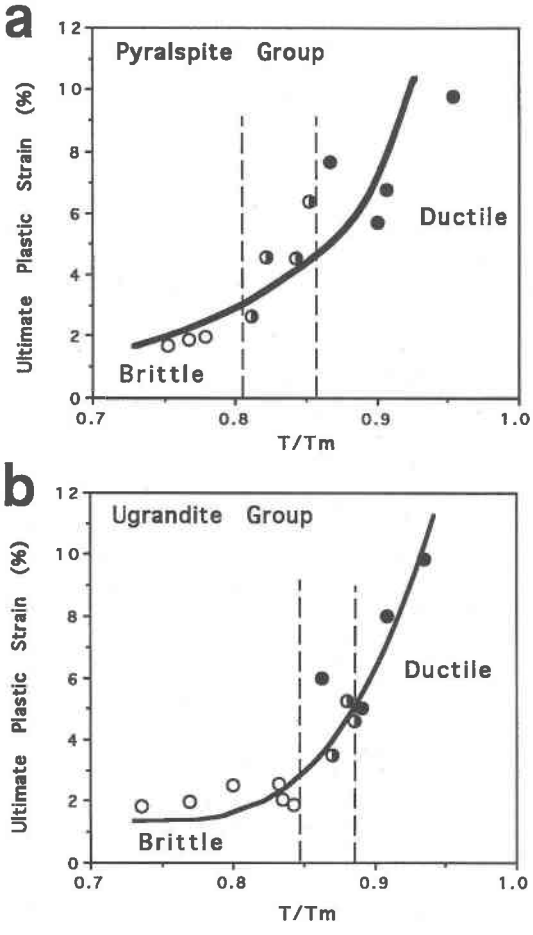

FIG. 5. Ultimate plastic strains of silicate garnets are plotted as a function of normalized temperature (T/T_m) to show the brittle–ductile transition. The ultimate strain is defined as permanent strain measured at the point where the sample fails. For samples deformed in ductile flow, the ultimate strain is referred to the permanent strain measured at the end of experiment. Open symbols stand for fractured samples with $\varepsilon_p < 3\%$ (brittle), half-open symbols, for fractured samples with $\varepsilon_p = 3$–5% (semi-brittle), and solid symbols, for samples without fracturing at the end of experiment with $\varepsilon_p > 5$–8% (ductile). Dashed lines show schematically the temperatures range of the brittle–ductile transition. (a) Pyralspitic garnet group, (b) ugranditic garnet group.

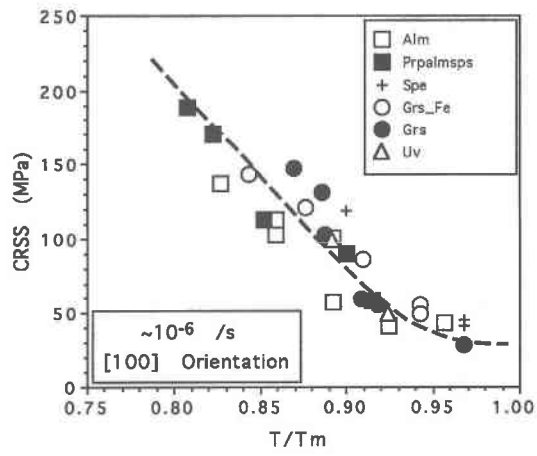

FIG. 6. Critical resolved shear stress (CRSS) as a function of normalized temperature (T/T_m) for ½<111> slip system, calculated from the yield stress at a strain rate of $1–3 \times 10^{-6}$/s. Garnet crystals were compressed along the [100] direction. Dashed line is drawn to show the general variation of the CRSS with T/T_m.

Although the transition region is broad between purely brittle and ductile behaviors, we can, based on the observed modes of failure and ε_p, classify the deformation of silicate garnets into three regimes: brittle regime (fracture occurs at $\varepsilon_p < 3\%$), semi-brittle regime (fracture occurs at an ε_p of 3–5%) and ductile regime ($\varepsilon_p > 6\%$, or no fracture observed at the end of experiment). The general pattern is comparable among silicate garnets studied, but the boundary conditions (T and ε) vary from one case to the other. To constrain the transition conditions, the data within the semi-brittle regime for all silicate garnets were compiled and fitted to an empirical equation

$$T_c = T_m[A + B \log(\dot{\varepsilon})] \quad (2)$$

where T_c is the critical temperature for the brittle–ductile transition at a given strain-rate ($\dot{\varepsilon}$); A and B are two constants that are experimentally determined as 1.043 ± 0.032 and 0.030 ± 0.001, respectively. Experimental results suggest that crystals of garnet are brittle if deformed at $T < T_c = T_m[1.011 + 0.031 \log(\dot{\varepsilon})]$, but ductile at $T > T_c = T_m[1.075 + 0.029 \log(\dot{\varepsilon})]$. These conditions are considered as the brittle – semi-brittle and semi-brittle – ductile boundaries in the deformation spectrum of silicate garnets.

We further studied the mechanical data obtained within ductile regime to establish a flow law for silicate garnets. The data from samples reaching steady-state creep were analyzed by applying the least-squares fit to a power-law creep equation; the result is given as

$$\dot{\varepsilon} = A\left(\frac{\sigma}{\mu}\right)^n \exp\left(-g\frac{T_m}{T}\right), \quad (3),$$

in which $\log_e A\ (s^{-1}) = 40.1 \pm 5.6$, $n = 3.0 \pm 0.5$ and $g = 32 \pm 2$; σ is the flow stress at steady-state creep, μ is shear modulus, T_m and T are the melting and experimental temperatures, respectively (both in K).

Microstructures

Optical observations

Oblique shear fractures through the entire crystal were observed in samples deformed in the brittle regime. We recovered a few samples by unloading immediately after the yield point. Little evidence of plastic deformation was observed, except for diffusive undulatory extinction at tips of microcracks. Microcracks, inclined at an angle of ~40°–45° towards σ_1, were observed, which obviously are aligned along the crystallographic orientation of <110>. We believe that the final failure of crystals is related to the initiation, propagation and connection of these microcracks.

Optical micrographic images of Prpalmsps, deformed in transitional (Prpalmsps: sample 4–d11) and ductile regimes (Prpalmsps: sample 8–d20) are shown in Figures 7 and 8. Sample 4–d11 shows extensive undulatory extinction and slip bands due presumably to heterogeneous deformation (Fig. 7). A local concentrated slip band (A in Fig. 7), not observed in the starting crystal and confirmed due to activation of dislocations in GGG garnet (Wang *et al.* 1996a), is one of the common features. We further noticed that microcracks, at an angle of 40°–45° toward σ_1, were initiated from a place where slip bands were of higher density (B in Fig. 7). Microcracks and slip bands are spatially coincident, which indicates a strong interaction between dislocation motion and microcracks. A local high concentration of stress due to pile-up of dislocations is very likely responsible for nucleation of microcracks. Compared with the sample deformed to a large strain (Prpalmsps: sample 8–d20, $\varepsilon_p = 9.0\%$), the undulatory extinction seen in Prpalmsps, sample 4–d11 is rather diffuse, whereas better organized band-like structures occur in Prpalmsps, sample 8–d20 (Fig. 8). No microcracks were seen in this sample at the optical scale. The high ductility of Prpalmsps, sample 8–d20 is consistent with intense activity of dislocations, in which pervasive and homogeneously distributed dislocations (Fig. 9), revealed by surface chemical etching, were observed. The band-like features, observed in all six silicate garnets, form orthogonal sets cross-cutting each other at 90°, suggesting {110} as the dominant glide planes of the dislocations activated.

Dislocation structures

Only foils cut from samples deformed in semi-brittle and ductile regimes were examined with the TEM. Dislocation structures, in general, are comparable among the various silicate garnets. They are also similar to those observed in oxide garnets (Karato *et al.* 1995, Wang *et al.* 1996a). The majority of the dislocations, observed in samples deformed in the transition regime, are short and straight free dislocations, with projected dislocation-line directions dominantly subparallel to [100] (A in Fig. 10a). The distribution of these dislocations is rather homogeneous, with an average density of ~6 (±3) × $10^{11}/m^2$. There is no sign of dislocation

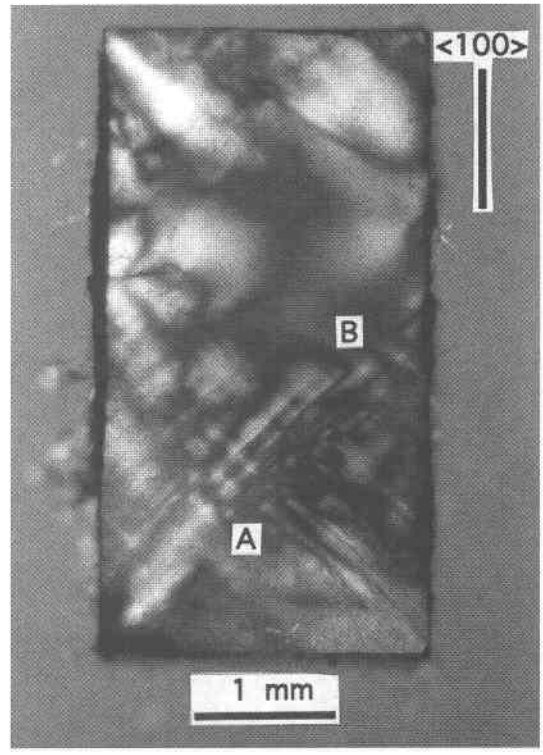

FIG. 7. Optical micrography of pyralspitic garnet (sample Prpslmsps 4–d11) deformed at 1423 K and 5.4 × 10^{-7}/s, ε = 5%. Crossed nicols. The direction of compression is parallel to [100]. Deformation is localized along oblique slip bands (A). Microcracks initiated at the tips of slip bands (B). Observed microcracks follow the crystallographic orientation <110>.

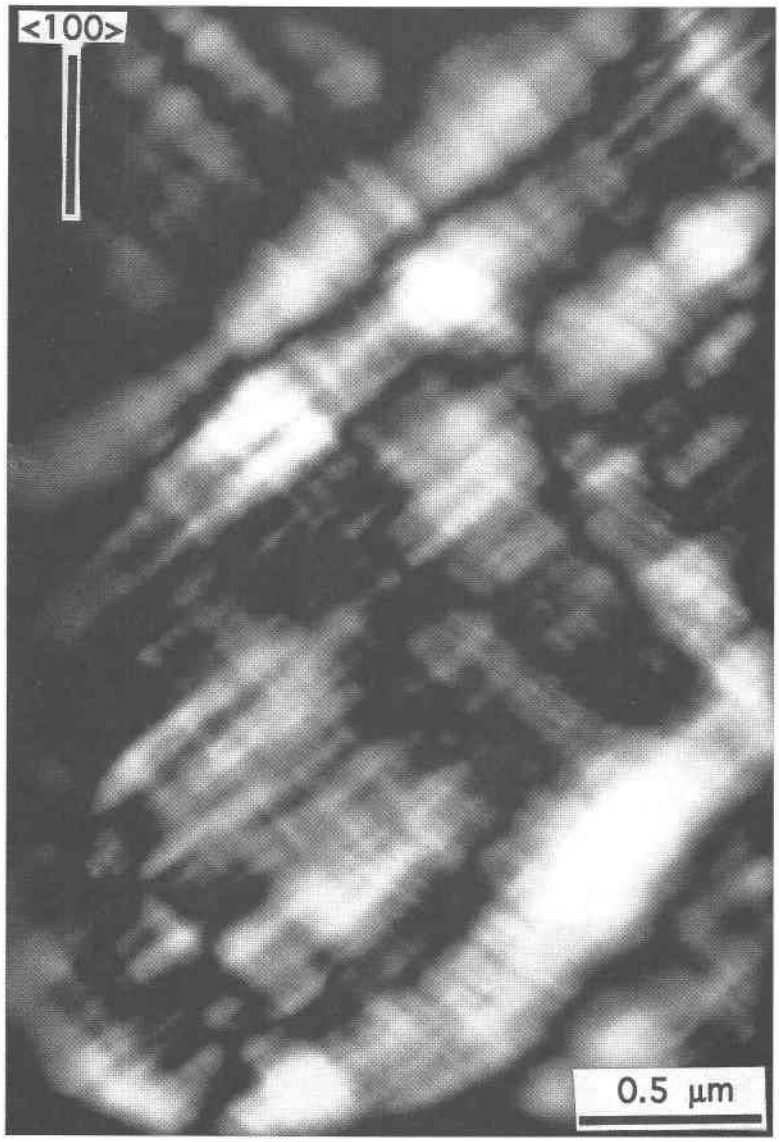

FIG. 8. Optical micrography of pyralspitic garnet (sample Prpalmsps 8–d20) deformed at 1423 K and 5.4×10^{-7}/s, $\varepsilon_p = 9\%$. Crossed nicols. The direction of compression is parallel to [100]. Deformation is homogeneous, with well-organized band-like structures (orthogonal sets cross-cutting each other at 90°) along the slip planes {110}. No oblique macrocracks were observed at the end of the run.

entanglement, but local high density of dislocations was occasionally seen. Using the conventional image-contrast method, we infer that the Burgers vector for the dominant free dislocation is $\mathbf{b} = \frac{1}{2}\langle 111 \rangle$, which is at a large angle (>80°) to its projected dislocation-line direction. Hence this set of dislocations is of edge character. We did not see substantial variations in dislocation substructures among samples in the transition regime, but we did observe some distinct dislocation substructures in the samples deformed to a large strain in the ductile regime at higher temperature. (1) Dislocation lines appeared to change direction from place to place, suggesting a variation in types of dislocation, edges *versus* screws. For example, note dislocation A and dis-

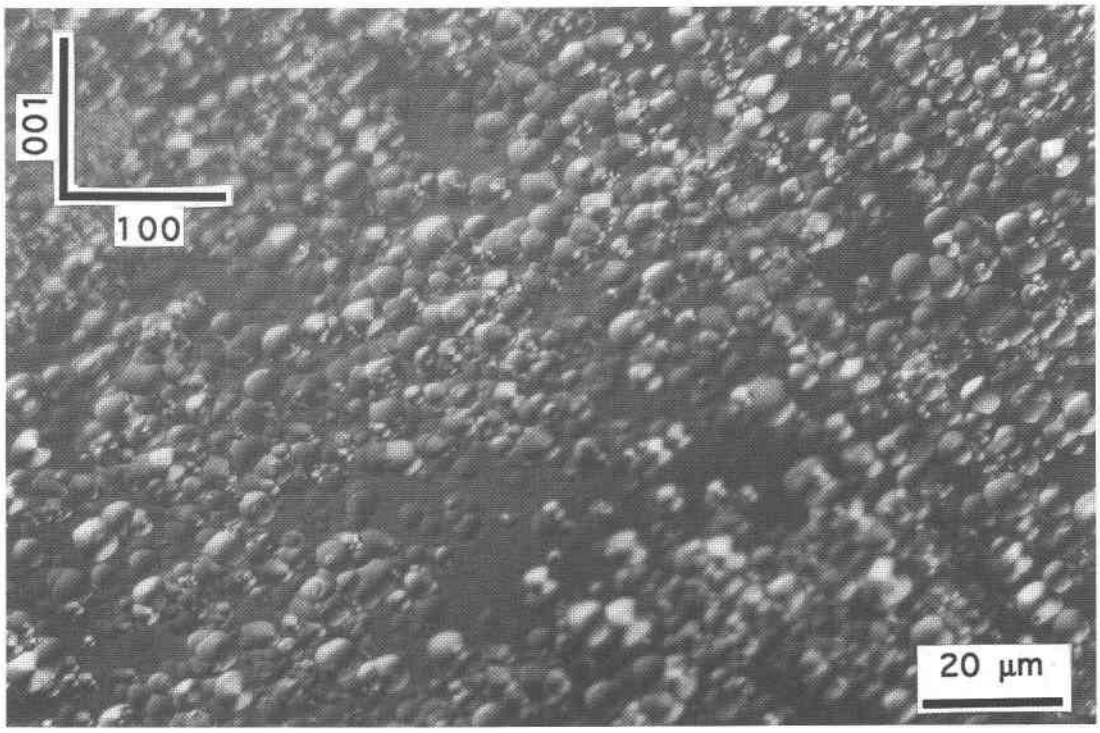

FIG. 9. Optical micrography showing the distribution of dislocations, revealed by chemical etching, in sample Prpalmsps 8–d20 deformed at 1423 K and 5.4 × 10^{-7}/s, ε_p = 9%

location B seen in Figure 10b. (2) Triple junctions were commonly observed (C and D in Fig. 10b). We did not perform a detailed TEM analysis on the nature of the triple junction, but assumed that it is due to dislocation interaction such as ½ <111> + ½ <$\bar{1}\bar{1}$1> = <001>, which was observed as dominant interaction in GGG garnet (Wang *et al.* 1996a). The occurrence of triple junctions indicates the operation of multiple slip systems. (3) Dislocation arrays and irregular networks were found to be rare, but present (E in Fig. 10b). We also saw dislocation loops ~0.1–0.5 μm in size in samples deformed in ductile regimes (C in Fig. 10a), which represent the motion of dislocation through climb.

TEM observations on dislocation substructures of deformed garnets suggest an intensive activation of dislocations with different Burgers vectors in ductile regime. Multiple processes could be involved in the steady-state deformation of silicate garnets, but dislocation glide is considered to be the dominant process. Determining physical mechanisms that are rate-controlling in the deformation of garnet is essential, but a detailed analysis and discussion require substantial work and are beyond the scope of this paper.

DISCUSSION

Crystal plasticity of silicate garnets at high temperature

Various processes of deformation may be responsible for ductile behavior of rocks and minerals, which are classified into three categories in terms of physical basis (*e.g.*, Paterson 1978): cataclastic flow, crystal plasticity and diffusion flow. In a broad sense, the brittle–ductile transition through crystal plasticity is expected to be the predominant mechanism under conditions of high pressure and high temperature as intergranular deformation is greatly suppressed (Mogi 1972, Horii & Nemat-Nasser 1986). The nature of the brittle–ductile transition through crystal plasticity can be studied by investigating the onset of significant plastic deformation as a function of temperature and strain rate in a single crystal, which is the approach employed in this study.

The term "crystal plasticity" is used to cover the permanent deformation (pure plastic strain) of crystalline material produced by twinning and dislocation slip.

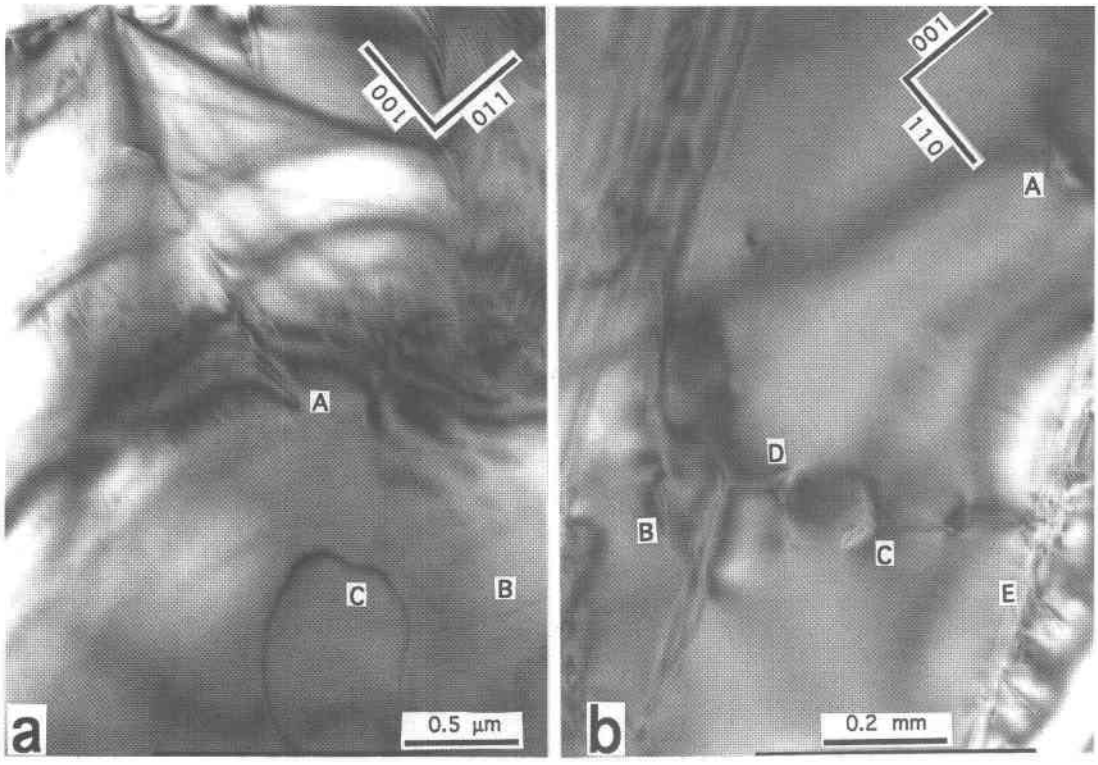

FIG. 10. (a) A TEM bright field image of grossular (Grs 6–d12, deformed at T = 1398 K and 5.6×10^{-7}/s, $\varepsilon_p = 8.2\%$. Straight free dislocations (A) with **b** = (½)[111]. (b) A TEM bright-field image of almandine (Alm 5–d17, deformed at T = 1423 K and 1.6×10^{-5}/s, $\varepsilon_p = 7.5\%$). Short and curved free dislocations with varying dislocation-line directions (A and B). Triple junctions (C and D) formed by the dislocation interaction and irregular array of dislocations (E).

Twinning is insignificant in the deformation of silicate garnets at high temperature, as no substantial twinning-induced strain was seen. Dislocation slip occurs by either glide (propagating on its slip plane) or climb (propagating perpendicular to its slip plane) depending on crystal structure and conditions of deformation. One of the most fundamental questions in (high-temperature) plasticity is the relative role of dislocation multiplication and migration (Weertman 1968, Poirier 1976, Takeuchi 1989, Wang *et al.* 1996b). Both multiplication and migration of dislocations are necessary to maintain steady-state creep; the slower of the two processes will determine the overall rate of steady-state creep. Migration of dislocations can be achieved through either glide or climb; the slower one, again, will control the overall rate of creep where they are sequential processes. Both climb-controlled and glide-controlled creep have been reported in rocks and minerals (Nicolas & Poirier 1976, Karato *et al.* 1995); the critical issue is the dominant resistance to dislocation slip (Hirth 1983). Creep of crystals is, in general, rate-controlled by dislocation glide where intrinsic resistance (the Peierls stress) is dominant, and oxide garnets provide a good example (Rabier & Garem 1984, Karato *et al.* 1994).

Mechanical data, obtained in this study, demonstrate clearly that silicate garnets can be deformed plastically as long as the temperature and strain rates are satisfied. Furthermore, both mechanical data and deformation substructures suggest that dislocation glide is the most important mechanism contributing to the plasticity of silicate garnets at high temperature. (1) Twinning is rare and insignificant to the creep of silicate garnets at the conditions of this study. (2) Well-developed conjugate shear-bands are common features in most garnet crystals deformed at $T > 0.9\ T_m$; these are identified as resulting from the intensive gliding of dislocations with **b** = ½<111> along the {110} planes (slip system: ½<111>{110}). (3) The dominant dislocations are free dislocations, and relative straight with projected line-directions parallel to each other. This pattern of dislocation suggests a high Peierls potential so that dislocation glide is difficult. (4) Weak evidence for dislocation climb was found in most of the deformed crystals of garnet, which suggests either that dislocation

climb is easier or the contribution from dislocation climb to the total plastic strain is limited.

Variation of the CRSS (for ½<111> slip system) with temperature provides additional support for the importance of dislocation glide. Measured CRSS reached the lowest value at ~0.9 T_m, suggesting that the energy barrier (the Peierls potential) to be overcome by dislocation glide is effectively lowered at this temperature. Enhancement in plastic strain at 0.8–0.9 T_m should be associated with intensive activity of dislocation glide, resulting from the decrease in CRSS (see Figs. 5 and 6). Additional support comes from the result of stress-dip tests performed on oxide garnets (Karato *et al.* 1995). The stress-dip test is a powerful tool for determining the relative role of the dislocation glide *versus* dislocation climb by determining the magnitude of internal stress (Takeuchi 1989). The ratio σ_i/σ is found to be unusually low for oxide garnets ($\sigma_i/\sigma < 0.8$, σ_i: internal stress, σ: applied stress, Karato *et al.* 1995, Wang *et al.* 1996a), implying a dominant role of dislocation glide in controlling the rate of creep. Considering the facts that both oxide and silicate garnets have the same structures and comparable unit-cell dimensions (hence the similar dislocation-slip system and resistance to creep), and that they belong to an isomechanical group (Karato *et al.* 1995), the result of the stress-dip test obtained on oxide garnets can be applied to silicate garnets.

Observed deformation-induced microstructures and macromechanical data are consistent with a glide-controlled model for silicate garnets. We therefore conclude that plastic deformation of silicate garnets under the conditions of this study is produced dominantly by dislocation glide. The high creep strength is due to the large resistance to dislocation glide, which can be interpreted in terms of the body-centered-cubic (b.c.c.) structure and large unit-cell of silicate garnets. We note that experimentally deformed silicate garnets show dislocation structures differing from those preserved in naturally deformed silicate garnets, in which subgrain boundary, well-organized dislocation array and cell structure are frequently observed. This discrepancy may be explained as follows. (1) The total amount of plastic strain of experimentally deformed silicate garnets (<15%) was limited by the experimental time-scale. Dislocation structures related to recovery processes can be effectively formed only at a large plastic strain ($\varepsilon_p > 30\%$), in particular where creep is rate-controlled by dislocation glide. (2) Dislocation climb is much easier than dislocation glide under the conditions of this study, so that the dislocation structures related to glide are better preserved. In fact, diffusion rates of cations in silicate garnets are not very slow (Kretz 1966, 1974, 1994), implying easy recovery (Karato *et al.* 1995). (3) Microstructures of naturally deformed silicate garnets may reflect the effect of static annealing, as suggested by Karato *et al.* (1995). We suggest that shear deformation, which makes the large plastic strain possible, should be conducted on silicate garnets to reach a better understanding of the discrepancy in dislocation substructures between experimentally and naturally deformed silicate garnets.

Applicability to polycrystalline aggregate of silicate garnets

It is important to note that here we are only dealing with the role of crystal plasticity in brittle–ductile transition of silicate garnets, and describe the onset of crystal plasticity as a function of temperature and strain rate. Caution must be taken for the transition conditions of silicate garnets in nature, as cataclastic flow and diffusion flow (grain-boundary sliding) are also common in nature. Cataclastic flow results from microcracking and relative movement of the fragments. It occurs in shallow parts of the Earth (lower T and P), where friction between the sliding parts is possible. In the deep interior of the Earth, where frictional sliding is effectively suppressed by pressure, the brittle–ductile transition occurs mainly through either diffusion flow or crystal plasticity, depending critically on grain size (Paterson 1976, Karato & Wu 1993). We believe that dislocation creep is dominant in a large part of the lower crust and the upper mantle, except where grain-size reduction is significant. The dominance of crystal plasticity in the lower crust and the upper mantle is supported by widely observed seismic anisotropy, which exclusively results from LPO (lattice preferred orientation) due to dislocation slip. Thus we believe that a brittle–ductile transition occurring *via* crystal plasticity may be common in the lower crust and the upper mantle.

We propose further that the results obtained on single crystals are applicable to polycrystalline aggregates in natural eclogites and garnetites based on the crystal structures and the availability of dislocation-slip systems in silicate garnets. In order to deform a polycrystalline aggregate by crystallographic slip, various slip systems are required to allow necessary degree of freedom. In accordance with the criterion of von Mises (Groves & Kelly 1963), five independent slip systems are required to satisfy the displacement compatibility at grain boundaries for an arbitrary change in shape. Experimental results on garnets show that ½<111>{1$\bar{1}$0} and <100>{010} slip systems can be activated at the conditions of this study (Garem *et al.* 1982, Rabier & Garem 1984, Karato *et al.* 1995, Wang *et al.* 1996a), which provide a total of 12 equivalent slip systems. Even though it has been found that **b** = <100> dislocations are more difficult to activate than **b** = (½)<111> dislocations, ½<111>{1$\bar{1}$0} alone can provide five independent strain components, which are sufficient to deform polycrystalline aggregates homogeneously. The availability of slip systems will keep the deformation of polycrystalline aggregates from grain-boundary hardening, so that the brittle–ductile transition of polycrystalline garnet can be realized merely by crystal plasticity.

To be conservative, we suggest that the transition boundary defined by crystal plasticity can be taken as the upper bound of the transition boundary for polycrystalline aggregates. The lower bound should be defined by either cataclastic and diffusion flow, which is still unknown. A lower temperature of the transition is also expected in nature if crystal plasticity of garnet is affected significantly by extrinsic factors such as the presence of H_2O, which could be significant, as demonstrated for olivine and other minerals (*e.g.*, Hirth & Kohlstedt 1996).

Geological implications

One direct application of this study is to estimate the geological conditions under which the brittle–ductile transition of natural silicate garnets may occur. In Figure 11, we compare the data of silicate garnets deformed naturally and experimentally. It appears that the transition boundaries determined in laboratory experiments can be linearly extrapolated to the geological conditions in T/T_m – $\log(\dot{\varepsilon})$ space. This implies that crystal plasticity controls the brittle–ductile transition in nature as well.

Garnet-group minerals showing signs of ductile deformation are commonly observed in various P–T conditions (metamorphic grade) in nature; we believe that the bulk composition of the garnet is an important variable. Figure 12 is calculated from empirical equation (2) and shows the transition temperature for various garnet compositions as a function of strain rate. Different garnet compositions have different melting temperatures and accordingly different critical temperature for the transition. At a strain rate of 10^{-14}/s, which is typical for shear zones in the crust, most types of garnet can be deformed plastically at temperature above 1023–1223 K depending on bulk composition. Such a high temperature can occur in certain granulite-facies metamorphic rocks, such as those in the Morin shear zone, Grenville tectonic province (Ji & Martignole 1994, 1996) and in the Highland Complex of Sri Lanka (Kleinschrodt & McGrew 1995). At lower strain-rates (Figs. 12c–d), ductile deformation of garnets can appear even at lower temperatures ($T \approx 923$ K for Sps). This may be the case described by Dalziel & Bailey (1968) and Ross (1973).

Figure 13 plots the flow strengths of quartz, plagioclase, a pyralspitic garnet, olivine and pyrope as a function of temperature at a strain rate of 10^{-14}/s assuming that all these minerals deform within the dislocation regime. It is generally true that dislocation creep prevails in dry and coarse-grained (>50 μm) rocks, as indicated by the presence of a preferred crystallographic orientation, a shape fabric and optical and TEM evi-

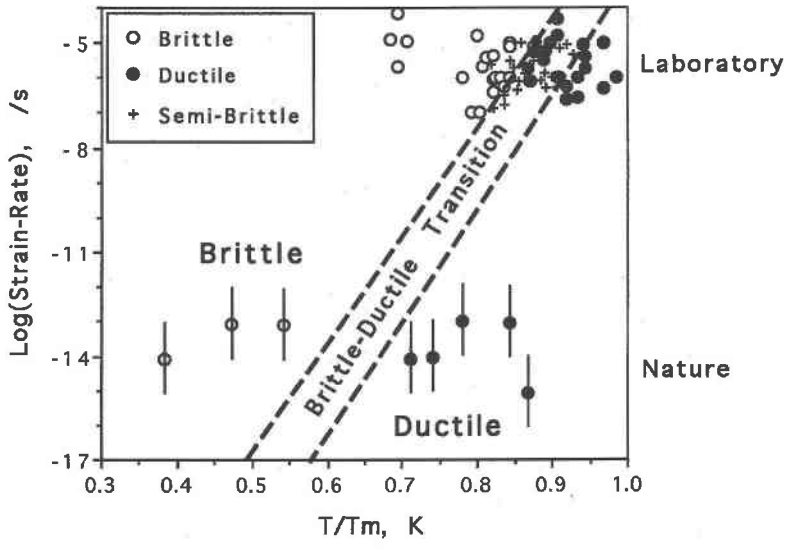

FIG. 11. Extrapolation of laboratory data to geological conditions, assuming that crystal plasticity is the dominant mechanism for the brittle–ductile transition. Open symbols stand for brittle deformation, solid symbols for ductile deformation, +, for semi-brittle deformation. Experimental data were taken from this study, and data on natural garnet were estimated from Ando *et al.* (1993), Bryhni (1966), Carstens (1969), Dalziel & Bailey (1968), Doukhan *et al.* (1994), Ji & Martignole (1994), Ji *et al.* (1997), Kleinschrodt & McGrew (1995) and Lappin (1967). Dashed lines mark the brittle–ductile transition zone for silicate garnets deformed either experimentally or naturally.

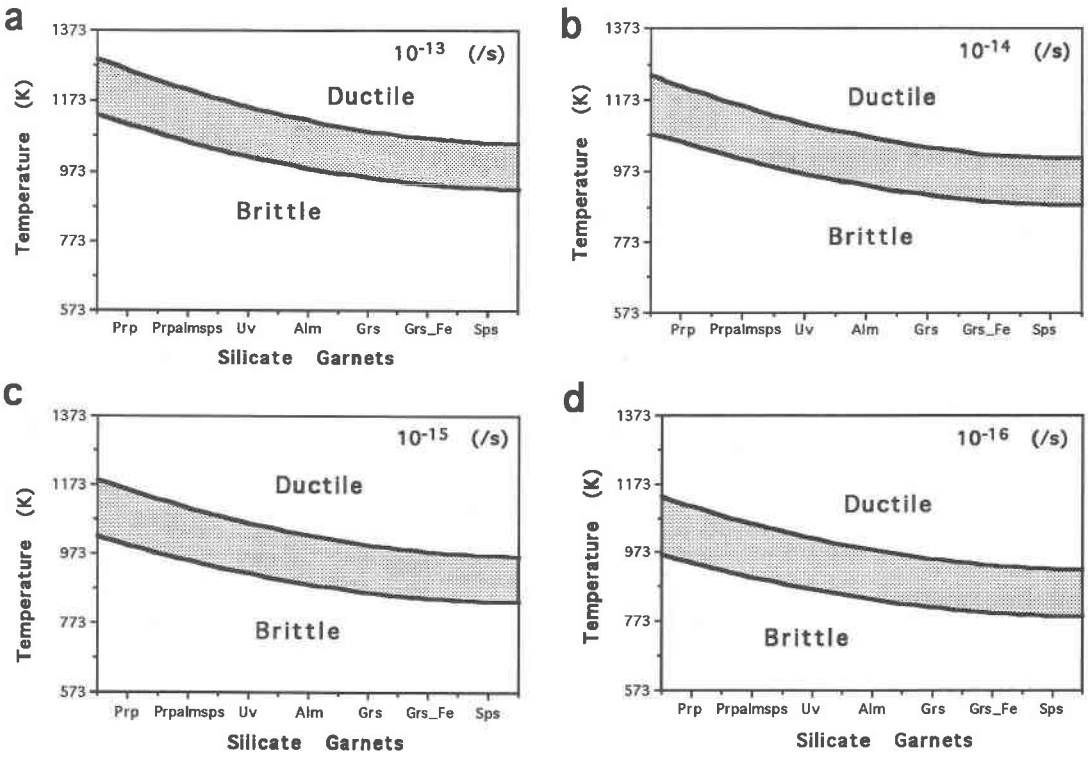

FIG. 12. The critical temperature for the brittle–ductile transition of garnets as a function of tectonic strain-rate (from 10^{-16} to 10^{-13}/s), calculated using empirical equation (2). The semi-brittle region is shaded.

dence of intracrystalline strain-induced microstructures. The curves shown in Figure 13 are calculated from flow laws for quartz (Gleason & Tullis 1995), plagioclase (Shelton & Tullis 1981), olivine (Chopra & Paterson 1981), pyralspitic garnet and pyrope (this study). In the crust, garnet ("pyralspite") is much stronger than quartz and feldspar at temperature lower than 1173 K, but the rheological contrasts between garnet and quartz and feldspar are minimal at temperature above 1173 K. This agrees with the observations of Ji & Martignole (1994) and Kleinschrodt & McGrew (1995), carried out on granulite-facies mylonites. In the upper mantle, however, garnet (pyrope) is invariably about two orders of magnitude stronger than olivine, and the rheological contrast between these two minerals is almost constant. This inference also is consistent with the observations on naturally deformed garnet peridotites (Nicolas & Poirier 1976). Comparisons between the flow strengths of garnet and pyroxene or amphibole are impossible at this point since reliable flow-laws for pyroxene and amphibole are not available. Our experimental results suggest that most types of garnet in metamorphic rocks in the crust should deform in the brittle regime, and ductile deformation of garnet is expected only under extreme conditions, such as high temperature or low strain-rate (or both).

Another indirect application of this study concerns the relevance of garnet crystals as a mineral phase for geobarometry and geothermometry. The composition of a garnet coexisting with other minerals is a sensitive indicator of the metamorphic P–T path followed during mineral growth (Spear & Selverstone 1983). In addition, radiogenic isotopic ratios of garnet can provide valuable information about absolute ages and rates of tectonic and metamorphic processes (Christensen *et al.* 1989, Burton & O'Nions 1991). These applications are based on the assumption that garnet is a closed system after the formation and growth of the crystals. It is thus important to identify the physical conditions for brittle deformation of garnets. If garnet is fractured, it will no longer be a closed system, because the brittle fractures will serve as paths of fluids and mass diffusion and allow the garnet interior to react with matrix minerals and fluids. This makes a garnet an open system. As pointed out by Whitney (1996), "the results of quantitative petrologic applications that use garnet and mineral-inclu-

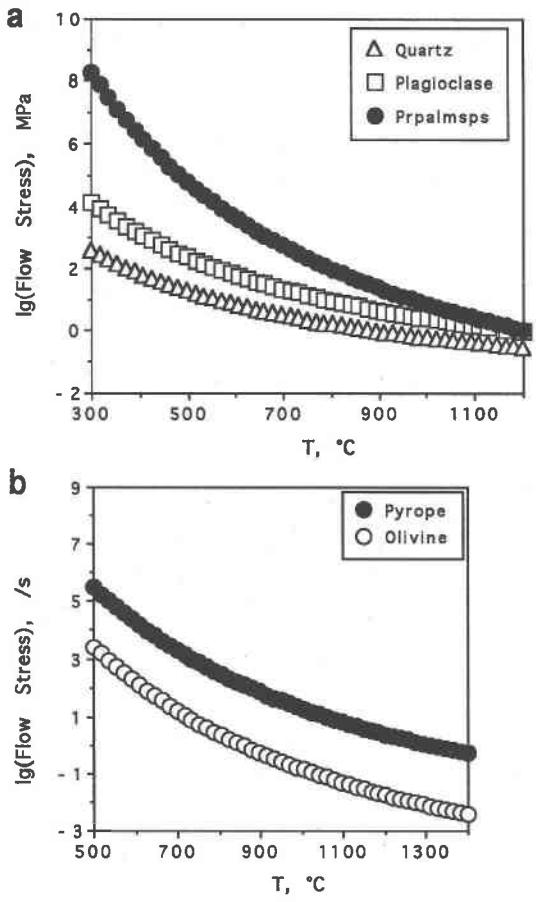

FIG. 13. Flow strength – temperature profiles in the dislocation creep regime for crustal garnet (Prpalmsps), quartz and plagioclase (a), upper mantle garnet (pyrope) and olivine (b) at a strain-rate of 10^{-14}/s. Thickness of the curves stands for the error range. The flow-law parameters for quartz, plagioclase and olivine are taken from Gleason & Tullis (1995), Shelton & Tullis (1981) and Chopra & Paterson (1981), respectively. The flow-law parameters for Prpalmsps and pyrope are taken from this study.

sion compositions will be affected if care is not taken to identify sites of modification so that specific garnet compositions can be linked to the processes that produced them." The determination of the brittle–ductile transition in deformation will provide the constraints for the applicability of P–T–t path determined from garnet crystals.

ACKNOWLEDGEMENTS

Major parts of the experimental works were finished during WZC's visits to University of Minnesota, the Institute of Geology, State Seismological Bureau of China, and GeoForchungsZentrum Potsdam. WZ thanks Drs. Shengzu Wang, Shun Karato and Georg Dresen for the use of their facilities, Shuqiang Li for helping with TEM observations. Discussions with Shun Karato were very much appreciated. Critical comments from Simon Hanmer, Toby Rivers, Robert F. Martin and an anonymous reviewer helped to improve the quality of the paper. We thank NSERC and FCAR funds for financial support.

REFERENCES

ANDO, J., FUJINO, K. & TAKESHITA, T. (1993): Dislocation microstructures in naturally deformed silicate garnets. *Phys. Earth Planet. Interiors* **80**, 105-116.

BLUMENTAL, W.R. & PHILLIPS, D.S. (1996): High-temperature deformation of single-crystal yttrium–aluminum garnet (YAG). *J. Am. Ceram. Soc.* **79**, 1047-1052.

BRYHNI, I. (1966): Reconnaissance studies of gneisses, ultrabasites, eclogites and anorthosites in outer Nordfjord, western Norway. *Norges geol. undersokelse* **241**, 1-68.

BURTON, K.W. & O'NIONS, R.K. (1991): High-resolution garnet chronometry and the rates of metamorphic processes. *Earth Planet. Sci. Lett.* **107**, 649-671.

CARSTENS, H. (1969): Dislocation structures in pyropes from Norwegian and Czech garnet peridotites. *Contrib. Mineral. Petrol.* **24**, 348-353.

_____ (1971): Plastic stress relaxation around solid inclusions in pyrope. *Contrib. Mineral. Petrol.* **32**, 289-294.

CHOPRA, P.N. & PATERSON, M.S. (1981): The experimental deformation of dunite. *Tectonophys.* **78**, 453-473.

CHRISTENSEN, J.N., ROSENFELD, J.L. & DE PAOLO, D.J. (1989): Rates of tectonometamorphic processes from rubidium and strontium isotopes in garnet. *Science* **244**, 1465-1469.

CORMAN, G.S. (1990): Creep of oxide single crystals. *Materials Laboratory, Wright Research and Development Center, Air Force System Command, Wright-Patterson Air Force Base, Ohio, Final Rep.* **86**.

DALZIEL, I.W.D. & BAILEY, S.W. (1968): Deformed garnets in a mylonitic rock from the Grenville Front and their tectonic significance. *Am. J. Sci.* **266**, 542-562.

DOUKHAN, N., SAUTTER, V. & DOUKHAN, J.C. (1994): Ultradeep, ultramafic mantle xenoliths: transmission electron microscopy preliminary results. *Phys. Earth Planet. Interiors* **82**, 195-207.

DRURY, M.R. & FITZ GERALD, J.D. (1997): Mantle rheology: insights from laboratory studies of deformation and phase transition. *In* The Earth's Mantle, Composition, Structure, and Evolution (I. Jackson, ed). Cambridge University Press, New York, N.Y. (503-559).

EVANS, B., FREDRICH, J.T. & WONG, TEN-FONG (1990): The brittle to ductile transition in rocks: recent experimental and theoretical progress. *In* The Brittle–Ductile Transition – the Head Volume (A.G. Duba, W.B. Durham, J.W. Handin & H.F. Wang, eds.). *Am. Geophys. Union, Geophys. Monogr.* **56**, 1-20.

GAREM, H., RABIER, J. & VEYSSIERE, P. (1982): Slip systems in gadolinium gallium garnet single crystals. *J. Mater. Sci.* **17**, 878-884.

GLEASON, G.C & TULLIS, J. (1995) A flow law for dislocation creep of quartz aggregates determined with the molten salt cell. *Tectonophys.* **247**, 1-23.

GREGG, W. (1978): The production of tabular grain shapes in metamorphic rocks. *Tectonophys.* **49**, T19-T24.

GROVES, G.W. & KELLY, A. (1963): Independent slip systems in crystals. *Philos. Mag.* **8**, 877-887.

HEARD, H.C. (1960): Transition from brittle fracture to ductile flow in Solenhofen limestone as a function of temperature, confining pressure, and interstitial fluid pressure. *In* Rock Deformation (D. Griggs & J. Handin, eds.). *Geol. Soc. Am., Mem.* **79**, 193-226.

_____ & CARTER, N.L. (1968): Experimentally induced "natural" intragranular flow in quartz and quartzite. *Am. J. Sci.* **266**, 1-42.

HIRTH, G. & KOHLSTEDT, D.L. (1996): Water in the oceanic upper mantle: implications for rheology, melt extraction and the evolution of the lithosphere. *Earth. Planet. Sci. Lett.* **144**, 93-108.

HIRTH, J.P. (1983): Dislocation. *In* Physical Metallurgy (third, revised and enlarged edition, R.W. Cahn & P. Haasen, eds.). North Holland, Amsterdam, The Netherlands (1223-1258).

HORII, H. & NEMAT-NASSER, S. (1986): Brittle failure in compression: splitting, faulting and brittle–ductile transition. *Philos. Trans., R. Soc. London* **319**, 337-374.

INGRIN, J. & MADON, M. (1995): TEM observations of several spinel–garnet assemblies: toward the rheology of the transition zone. *Terra Nova* **7**, 509-515.

JI, SHAOCHENG & MARTIGNOLE, J. (1994): Ductility of garnet as an indicator of extremely high temperature deformation. *J. Struct. Geol.* **16**, 985-996.

_____ & _____ (1996): Ductility of garnet as an indicator of extremely high temperature deformation: reply. *J. Struct. Geol.* **18**, 1375-1379.

_____, WANG, ZICHAO & SARUWATARI, K. (1998): Plasticity of eclogite: implications for rheology and seismic reflectivity of the subducting slab. *LITHOPROBE Rep.* **64**, 86-91.

_____, ZHAO, P. & SARUWATARI, K. (1997): Fracturing of garnet crystals in anisotropic metamorphic rocks during uplift. *J. Struct. Geol.* **19**, 603-620.

KARATO, S., WANG, ZICHAO & FUJINO, K. (1994): High-temperature creep of yttrium-aluminum garnet single crystals. *J. Mater. Sci.* **29**, 6458-6462.

_____, _____, LIU, B. & FUJINO, K. (1995): Plastic deformation of garnets: systematics and implications for the rheology of the mantle transition zone. *Earth Planet. Sci. Lett.* **130**, 13-30.

_____ & WU, P. (1993): Rheology of the upper mantle: a synthesis. *Science* **260**, 771-778.

KLEINSCHRODT, R. & MCGREW, A.J. (1995): Garnet plasticity in the lower continental crust: constraints on deformation mechanisms from microstructual and textural data. *J. Czech Geol. Soc.* **40**, 104.

KRETZ, R. (1966): Grain-size distribution for certain metamorphic minerals in relation to nucleation and growth. *J. Geol.* **74**, 147-173.

_____ (1974): Some models for the rate of crystallization of garnet in metamorphic rocks. *Lithos* **7**, 123-131.

_____ (1983): Symbols for rock-forming minerals. *Am. Mineral.* **68**, 277-279.

_____ (1994): *Metamorphic Crystallization.* John Wiley & Sons, New York, N.Y.

LAPPIN, M.A. (1967): Structural and petrofabric studies of the dunites of Almklovdalen, Nordfjord, Norway. *In* Ultramafic and Related Rocks (P.J. Wyllie, ed.). John Wiley & Sons, New York, N.Y. (183-190).

MEAGHER, E.P. (1982): Silicate garnets. *In* Orthosilicates (P.H. Ribbe, ed.). *Rev. Mineral.* **5**, 25-66.

MOGI, K. (1972): Fracture and flow of rocks. *Tectonophys.* **13**, 541-568.

NICOLAS, A. & POIRIER, J.P. (1976): *Crystalline Plasticity and solid State Flow in Metamorphic Rocks.* John Wiley & Sons, London, U.K.

PARTHASARATHY, T.A., MAH, T.I. & KELLER, K. (1992): Creep mechanism of polycrystalline yttrium–aluminum garnet. *J. Am. Ceram. Soc.* **75**, 1756-1759.

PATERSON, M.S. (1978): *Experimental Rock Deformation: the Brittle Field.* Springer-Verlag, Berlin, Germany.

POIRIER, J.P. (1976): On the symmetrical role of cross-slip of screw dislocations and climb of edge dislocations as recovery processes controlling high-temperature creep. *Revue de Physique Appliquée* **11**, 731-738.

RABIER, J. (1979): *Dissociation des dislocations dans les oxydes de structures grenat: application a l'étude de la deformation plastique du grenat de fer et d'yttrium (YIG).* Thèse de doctorat, Univ. de Poitiers, Poitiers, France.

_____ & GAREM, H. (1984): Plastic deformation of oxides with garnet structure. *In* Materials Science Research **18**

(R.E. Tressler & R.C. Bradt, eds.). Plenum Press, New York, N.Y. (187-198.)

_____, VEYSSIÈRE, P., GAREM, H. & GRILHE, J. (1979): Subgrain boundaries and dissociation of dislocations in yttrium iron garnet deformed at high temperatures. *Philos. Mag.* **A39**, 693-708.

_____, _____ & GRILHE, J. (1976): Possibility of stacking faults and dissociation of dislocations in the garnet structure. *Phys. Stat. Sol.* **A35**, 259-268.

RINGWOOD, A.E. (1991): Phase transformation and their bearing on the constitution and dynamics of the mantle, *Geochim. Cosmochim. Acta* **55**, 2083-2110.

ROSS, J.V. (1973): Mylonitic rocks and flattened garnets in the southern Okanagan of British Columbia. *Can. J. Earth Sci.* **10**, 1-17.

SHELTON, G.L. & TULLIS, J. (1981): Experimental flow laws of crustal rocks. *Eos, Trans. Am. Geophys. Union* **62**, 396 (abstr.).

SMITH, B.K. (1982): *Plastic Deformation of Garnets: Mechanical Behavior and Associated Microstructure.* Ph.D thesis, Univ. of California, Berkeley, California.

SPEAR, F.S. & SELVERSTONE, J. (1983): Quantitative P–T paths from zoned minerals: theory and tectonic applications. *Contrib. Mineral. Petrol.* **83**, 348-357.

TAKEUCHI, S. (1989): Motion of dislocations: characteristics of high-temperature deformation. *In* Rheology of Solids and of the Earth (S. Karato & M. Toriumi, eds.). Oxford University Press, Oxford, U.K. (3-14).

WANG, ZICHAO, BAI, Q., DRESEN, G., WIRTH, R. & EVANS, B. (1996b): High-temperature deformation of calcite single crystals. *J. Geophys. Res.* **101**, 20377-20390.

_____, KARATO, S. & FUJINO, K. (1996a): High temperature creep of single crystal gadolinium gallium garnet. *Phys. Chem. Minerals* **23**, 73-80.

WEERTMAN, J. (1968): Dislocation climb theory of steady-state creep. *Trans. Am. Soc. Metall.* **61**, 681-694.

WHITNEY, D.L. (1996): Garnets as open systems during regional metamorphism. *Geology* **24**, 147- 150.

WINCHELL, A.N. (1933): *Elements of Optical Mineralogy* (part II, 3rd ed.). John Wiley and Sons, New York, N.Y.

Received November 3, 1997, revised manuscript accepted October 15, 1998.